

Composition dependence of the ferroelectric-paraelectric transition in the mixed system $\text{PbZr}_{1-x}\text{Ti}_x\text{O}_3$

Beatriz Noheda, Noé Cereceda, Tomás Iglesias, Ginés Lifante, and Julio A. Gonzalo
Departamento de Física de Materiales, C-IV, Universidad Autónoma de Madrid, 28049 Madrid, Spain

Hui Ting Chen and Yong Ling Wang
Shanghai Institute of Ceramics, Chinese Academy of Sciences, 1295 Ding Xi Road, Shanghai 200050, China
(Received 30 January 1995)

The dielectric constant and losses of good quality ceramic samples of Nb-doped (1 wt % Nb_2O_5) $\text{PbZr}_{1-x}\text{Ti}_x\text{O}_3$ about the ferroelectric-paraelectric transition for $0.03 \leq x \leq 0.09$ have been measured with the aim of investigating the behavior of the thermal hysteresis with composition and the possible existence of tricritical points in this mixed system. The trend of the data, analyzed in terms of a generalized effective-field theory ($E_{\text{eff}} = E + \beta P + \gamma P^3 + \dots$) indicates that two tricritical points, at $x \cong 0.26$ and $x \cong 0.51$, are implied by the observed behavior at lower x .

The mixed system $\text{Pb}(\text{Zr}_{1-x}\text{Ti}_x)\text{O}_3$, abbreviated PZT, in which ferroelectric and antiferroelectric transitions were reported by Shirane and Suzuki,^{1,2} has been widely investigated because of its outstanding piezoelectric and pyroelectric properties. While the basic features of the ferroelectric phase diagram have been well known for a long time, little attention has been paid, as far as we know, to the composition dependence of the character (first or second order) of the ferroelectric-paraelectric transition. The character of the transition, and the possible existence of one or more tricritical points separating composition regions with discontinuous first-order transitions and continuous-second order transitions can be investigated, in good quality ceramic samples of varying composition, by means of simple dielectric constant and dielectric loss measurements. A decreasing trend with changing composition in the transition thermal hysteresis, or better in the difference between transition temperature (T^*) and extrapolated Curie temperature (T_c), is a clear indication that the system is approaching a tricritical point.

We report dielectric measurements in Nb-doped (1 wt % Nb_2O_5) PZT ceramics for $0.03 \leq x \leq 0.09$, prepared and sintered at 1340°C for 1.5 h at the laboratories of the Shanghai Institute of Ceramics, and for $x = 0.22$, kindly provided by Dr. W. Wersing (Siemens AG). A straightforward analysis of the data using a generalized effective-field approach, in which the standard molecular field $E_{\text{eff}} = E + \beta P$ is generalized³ to include higher-order terms, i.e., $E_{\text{eff}} = E + \beta P + \gamma P^3 + \dots$, leads to estimates of tricritical compositions at $x \cong 0.26$ and 0.51 , between which continuous (second-order) ferroelectric-paraelectric transitions are expected, the transitions^{4,5} corresponding to both ends, $x = 0$ and 1 , of the phase diagram being clearly discontinuous (first order). Interest in the ferroelectric properties of mixed lead zirconate/titanate ceramics has been boosted recently by the prospects of using PZT thin films in nonvolatile memories.⁶

The samples were thin disks (thickness ~ 1 mm, diame-

ter ~ 1 cm) cut from sintered and hot-pressed cylindrical samples with compositions $x = 0.03, 0.06, 0.08$, and 0.09 , doped with 1 wt% of Nb_2O_5 to improve the physical properties of the ceramics. A high-temperature furnace built at the Crystal Growth Laboratory of the UAM, Madrid, controlled by a Eurotherm Temperature Controller/Programmer with high-resolution ramp (model 903P/IS/HDV) was used. The samples were thermally treated by keeping them for several hours at temperatures of about 400°C before the measurements, and the slow heating and cooling rates employed were of the order of 20°C/h between room temperature and 400°C . The capacitance and dissipation factor were measured during the heating and cooling runs at regular intervals separated by about 0.1°C by means of an automatic Hewlett-Packard Bridge Precision LCR Meter (model 4284A) with an accuracy better than one part in 10^4 at a frequency of 1 kHz with a field amplitude of 8.3 V/cm.

Figure 1 depicts the inverse dielectric constant ϵ^{-1} vs

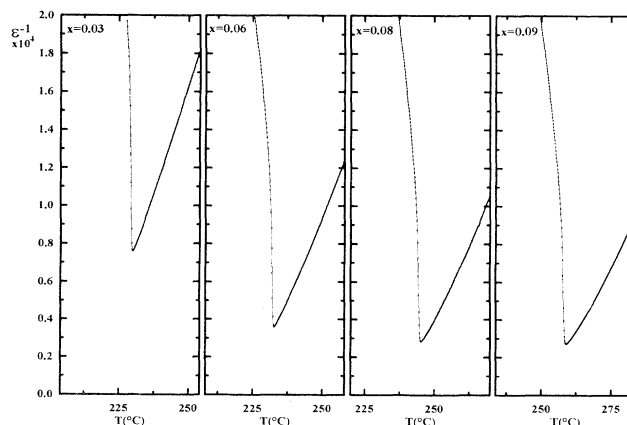


FIG. 1. Inverse dielectric constant ϵ^{-1} vs temperature near the ferroelectric-paraelectric transition for $\text{Pb}(\text{Zr}_{1-x}\text{Ti}_x)\text{O}_3$ doped with Nb (1 wt % Nb_2O_5) for various compositions in the range $0.03 \leq x \leq 0.09$.

temperature for $0.03 \leq x \leq 0.09$. The slope of ϵ^{-1} vs T above the transition temperature T^* is not equally well defined for all four compositions. This leads in some cases to deviations from the ideal Curie-law behavior due to differences in the compositional inhomogeneities, which causes uncertainties in the Curie temperature T_c extrapolated at $\epsilon^{-1} \rightarrow 0$. In all cases the slope was determined in an interval of about 20°C above T^* , taking into account numerically the derivative $d\epsilon^{-1}/dT$ and avoiding the rounded region usually observed immediately above T^* which increases for increasing x .

Figure 2 shows dielectric loss data $D = \tan\delta$ vs temperature for the same samples. It may be noted that, for $x=0.03$, no clearly defined peaks are observed, but well-defined discontinuous jumps mark the phase transition. The transition temperature T^* for increasing T is therefore well defined in every case by the dielectric loss data as well as by the dielectric constant data.

Table I gives results for T^* , T_c , and $\Delta T \equiv T^* - T_c$ for PZT compositions with $0.03 \leq x \leq 0.09$ and 1 wt% Nb_2O_5 as well as^{4,5} for PbZrO_3 ($x=0$), PbTiO_3 ($x=1$), and $x=0.22$, for later use. It can be seen that the trend of ΔT is decreasing with increasing x from $x=0.03$ to 0.22, for an estimate of ΔT has been obtained from the difference between $T(D_{\max})$ for increasing and decreasing temperature.

These results can be analyzed by means of a generalized effective-field theory in which the standard expression for the effective field³ in terms of the polarization,

$$E_{\text{eff}} = E + \beta P, \quad (1)$$

where $\beta = 4\pi T_c / C$ is a dimensionless coefficient depending on the geometry of the dipole lattice, is substituted by⁷

$$E_{\text{eff}} = E + \beta P + \gamma P^3 + \dots \quad (2)$$

With this substitution the equation of state relating P , E , and T ,

$$\frac{P}{N\mu} = \tanh \left[\frac{E_{\text{eff}}\mu}{k_B T} \right], \quad (3)$$

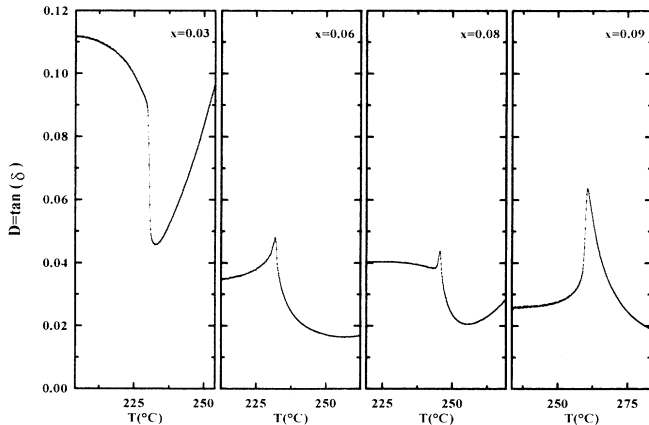


FIG. 2. Dielectric loss factor D vs temperature for the same samples as in Fig. 1.

TABLE I. Transition temperatures and Curie temperatures for $\text{Pb}(\text{Zr}_{1-x}\text{Ti}_x)\text{O}_3$ as a function of x . * = negligible. ΔT estimated from loss peaks.

x	Nb (%)	T^* (K)	T_c (K)	ΔT (K)
0	*	503	460	43.0
0.03	1	502.2	486.9	15.3
0.06	1	505.5	496.5	9.0
0.08	1	517.4	510.0	7.4
0.09	1	531.7	524.8	6.9
0.22	*	571.7		[1.7]
1.00	*	763	720	43

where N is the number of dipoles per unit volume, μ the elementary dipole moment, and k_B Boltzmann's constant, leads directly to

$$\frac{E}{\beta N\mu} = \left[\frac{T}{T_c} \right] \tanh^{-1} \left[\frac{P}{N\mu} \right] - \left[1 + (\gamma/\beta)(N\mu)^2 \left[\frac{P}{N\mu} \right]^2 \dots \right] \left[\frac{P}{N\mu} \right], \quad (4)$$

here $g \equiv (\gamma/\beta)(N\mu)^2$ is a second dimensionless coefficient which plays a decisive role in determining the character of the transition, g being $\frac{1}{3}$ being for a tricritical point (TCP) transition.

For a pure system the Curie temperature is given by

$$T_c = \beta N\mu^2 / k_B. \quad (5)$$

For a mixed system such as PZT, the composition-dependent Curie temperature $T_c(x)$ can be given in a first approximation⁸ in terms of the Curie temperatures of the components,

$$(T_c)_Z = T_c(0) = \beta_Z N_Z \mu_Z^2 / k_B, \quad (6)$$

$$(T_c)_T = T_c(1) = \beta_T N_T \mu_T^2 / k_B, \quad (7)$$

$$T_c(x) = T_c(0) \left[(1-x) + \left[\frac{\beta_T N_T \mu_T^2}{\beta_Z N_Z \mu_Z^2} \right] x \right] = T_c(1) \left[\left[\frac{\beta_Z N_Z \mu_Z^2}{\beta_T N_T \mu_T^2} \right] (1-x) + x \right], \quad (8)$$

where the ratio

$$\left(\frac{\beta_T N_T \mu_T^2}{\beta_Z N_Z \mu_Z^2} \right) = T_c(1) / T_c(0).$$

In our case we will assume that this ratio is not too sensitive to small amounts of doping, like 1 wt% Nb_2O_5 .

Similarly, the dimensionless coefficient g , which determines the phase transition character, and is given for a pure compound by

$$g = (\gamma/\beta)(N\mu)^2, \quad (9)$$

can be given for a mixed system in terms of the coefficients g of the components,

$$(g)_Z = g(0) = (\gamma_Z/\beta_Z)(N_Z\mu_Z)^2, \quad (10)$$

$$(g)_T = g(1) = (\gamma_T/\beta_T)(N_T\mu_T)^2, \quad (11)$$

as

$$g(x) = g(0) \left[(1-x)^2 + \left[\frac{\gamma_T/\beta_T}{\gamma_Z/\beta_Z} \right] \left[\frac{N_T\mu_T}{N_Z\mu_Z} \right]^2 x^2 \right]$$

$$= g(1) \left[\left[\frac{\gamma_Z/\beta_Z}{\gamma_T/\beta_T} \right] \left[\frac{N_Z\mu_Z}{N_T\mu_T} \right] (1-x)^2 + x^2 \right], \quad (12)$$

where the product of ratios

$$[(\gamma_T/\beta_T)/(\gamma_Z/\beta_Z)][(N_T\mu_T)^2/(N_Z\mu_Z)^2] = g(1)/g(0),$$

and we again expect that this product is not affected substantially by small amounts of doping with Nb.

As shown in previous work,⁹ within the framework of a generalized effective-field approach, the dimensionless quantities $T^*/T_c = 1 + \Delta T/T_c$, g , and $p_s^* = P_s(T^*)/P_s(0)$ are related among themselves by the relationships

$$T^*/T_c = 2[3 \tanh^{-1} p_s^*/p_s^* - (1-p_s^{*2})^{-1}]^{-1}, \quad (13)$$

$$g = [(T^*/T_c)(\tanh^{-1} p_s^*/p_s^*) - 1]/p_s^{*2}. \quad (14)$$

Numerical values for T^*/T_c and g as a function of p_s^* are given in Table II.

Figure 3 gives $\Delta T/T_c$ as a function of g in an extended range obtained by means of Eqs. (13) and (14). For $g \leq \frac{1}{3}$, i.e., below the TCP the transition is second order and no thermal hysteresis occurs under proper thermal equilibrium conditions. For $g > 0.4$ $\Delta T/T_c$ increases fairly rapidly. This relationship between $\Delta T/T_c$ and g will be used later to calculate ΔT for comparison with $(\Delta T)_{\text{obs}}$ as a function of x .

To analyze our PZT results we begin by fitting Eq. (8) to the data in Table I for $0.03 \leq x \leq 0.09$. We get

$$T_c(x) = T_c(0)[(1-x) + Ax]$$

$$A = 1.67, \quad T_c(0) = 476.9 \text{ K}. \quad (15)$$

This results in $T_c(0)$ and $T_c(1) = T_c(0)A$ values which can be compared with the Curie temperatures for the pure materials (no Nb) reported by other authors. The ratio^{4,5} $(T_c)_T/(T_c)_Z \cong 1.56$ is not far from $A = 1.67$ as anticipated.

Next we determine the relevant numerical parameters for Eq. (12). A reasonable fit is obtained for

$$g(x) = g(0)[(1-x)^2 + Bx^2],$$

$$B = 1.46, \quad g(0) = 0.534. \quad (16)$$

TABLE II. Numerical values for (T^*/T_c) and g as a function of $p_s^* \equiv P_s(T^*)/P_s(0)$.

p_s^*	(T^*/T_c) , Eq. (13)	g , Eq. (14)
0	1	$\frac{1}{3}$
0.35	1.0036	0.3910
0.40	1.0066	0.4131
0.45	1.0114	0.4415
0.50	1.0191	0.4783
0.55	1.0314	0.5276
0.60	1.0508	0.5944
0.65	1.0803	0.6829
0.70	1.1387	0.8387

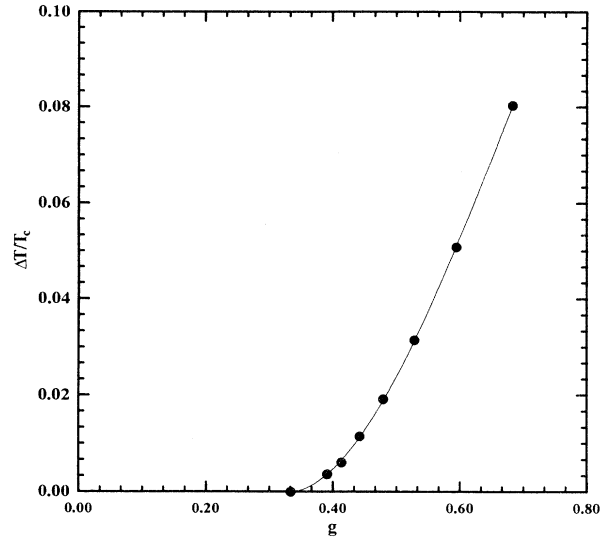


FIG. 3. Plot of $(\Delta T/T_c)$, where $\Delta T = T^*$ (transition temperature) $- T_c$ (Curie temperature), vs $g = (\gamma/\beta)(N\mu)^2$ (higher-order effective-field coefficient) after Eqs. (13) and (14).

Here, B and $g(0)$ have been estimated from the set of numerical values of $g(x)$ corresponding to $0.03 \leq x \leq 0.09$, using the $\Delta T/T_c$ values given in Table I and the graph in Fig. 3. It may be noted that $g(1) = g(0)B = 0.779$ so obtained is larger but not⁷ far from $(g)_T \cong 0.62$ at $T = T^*$, independently determined for the pure titanate according to Table I. On the other hand $g(0) = 0.534$ is somewhat

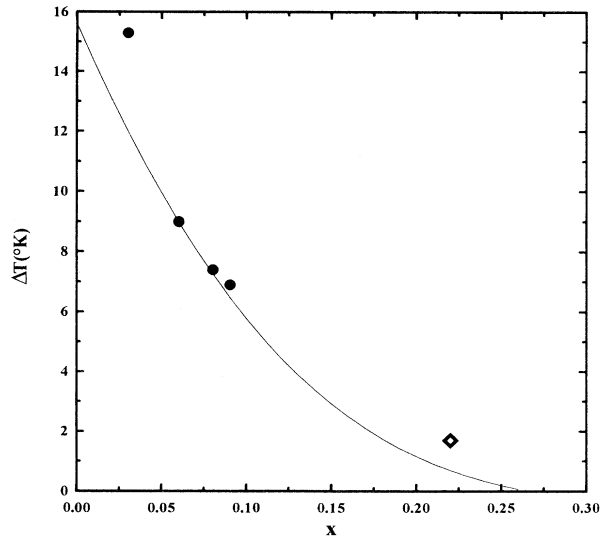


FIG. 4. $\Delta T = T^* - T_c$ vs x for $\text{Pb}(\text{Zr}_{1-x}\text{Ti}_x)\text{O}_3$. The curve is calculated from Eqs. (15) and (16) using the plot of $(\Delta T/T_c)$ vs g from Fig. 3, the solid circles are experimental points for $0.03 \leq x \leq 0.09$ (doped with 1 wt % Nb_2O_5), and \diamond is for $x = 0.22$ (estimated from the shift in D_{max} for heating and cooling runs). It is worth noticing that the experimental point for $x = 0.03$ appears to be further from the theoretical value than the rest. This may be due to the fact that $T_c(x)$ has a slightly different behavior in the low- x region $0 \leq x \leq 0.03$ (Ref. 8).

smaller than $(g)_Z=0.72$ at $T=T^*$ for the pure zirconate after Table I. The possibility that Nb doping slightly pushes some of the factors determining g for the titanate and the zirconate in opposite directions is not to be expected, *a priori*, but is not inconceivable.

Figure 4 shows the calculated curve for ΔT using Eq. (15) for $T_c(x)$ and Eq. (16) for $g(x)$ and the functional relationship between $\Delta T/T_c$ and g plotted in Fig. 3, together with $(\Delta T)_{\text{obs}}$ for $x=0.03, 0.06, 0.08$, and 0.09 (1 wt % Nb_2O_5 doped), and for $x=0.22$. A first tricritical point at $(x_{\text{TCP}})_1 \cong 0.26$ is indicated by the calculated curve, and a second one at $(x_{\text{TPT}})_2 \cong 0.51$ (not shown in the graph) is also deduced from the same equations for higher x values.

Thus we may conclude that a mixed ferroelectric sys-

tem like PZT can accommodate more than one tricritical point in a wide enough range of compositions. Recent theoretical work¹⁰ on ferroelectric solid solutions suggests that a detailed investigation of the lattice deformation through the transition may be useful to check the phase transition character of PZT solid solutions at x near the expected tricritical point compositions.

We would like to thank Gen Shirane for many informative discussions on structural aspects of this PZT system, and Wolfram Wersing for providing us the sample with $x=0.22$. The financial support of IBERDROLA (through Grant No. INDES/94) and CICYT (through Grant No. PB93-1253/94) is gratefully acknowledged.

¹G. Shirane and K. Suzuki, *J. Phys. Soc. Jpn.* **7**, 333 (1952).

²E. Swaguchi, *J. Phys. Soc. Jpn.* **8**, 615 (1953).

³J. A. Gonzalo, *Effective Field Approach to Ferroelectric Transitions and some Applications to Ferroelectrics* (World Scientific, Singapore, 1991).

⁴Z. Ujma and J. Handerek, *Acta Phys. Pol. A* **53**, 665 (1978).

⁵G. A. Samara, *Ferroelectrics* **2**, 277 (1971).

⁶S. L. Swartz and V. E. Wood, *Condens. Matter News* **1**, 5 (1992); J. F. Scott, J. Kammerdiner, M. Parris, S. Traynor, V.

Ottensbacher, A. Shawabkeh, and W. F. Oliver, *J. Appl. Phys.* **64**, 787 (1988).

⁷G. Lifante, J. A. Gonzalo, and W. Windsch, *Ferroelectrics* **146**, 107 (1993).

⁸B. Jaffe, W. R. Cook, and H. Jaffe, *Piezoelectric Ceramics* (Academic, New York, 1971), p. 136, Fig. 7.1.

⁹J. A. Gonzalo, R. Ramirez, G. Lifante, and M. Koralewski, *Ferroelectrics Lett.* **15**, 9 (1993).

¹⁰W. Windsch and H. Braeter, *Acta Phys. Pol.* **86**, 393 (1994).